Magnetic switching of the superconducting transition temperature in layered ferromagnetic/superconducting hybrids: Spin switch versus stray field effects

R. Steiner and P. Ziemann*
Abteilung Festkörperphysik, Universität Ulm, D-89069 Ulm, Germany
(Received 7 April 2006; published 14 September 2006)

The resistance and magnetization behavior of [ferromagnetic (FM)/superconducting (SC)/ferromagnetic (FM)] trilayers of the type (Co/Nb/Fe) was experimentally analyzed and related to their superconducting transition temperature T_c. As opposed to what is expected by proximity effect theory, T_c exhibited a minimum in case of an antiparallel relative orientation of the magnetization of the two sandwiching FM layers. Though this result is consistent with the predictions of spin-imbalance theory, additional experiments on exchange-biased CoO/Co/Nb/Fe systems revealed strong T_c changes, even for a fixed relative magnetization orientation of the FM layers pointing to stray fields, rather than magnetization orientations, as causing the observed T_c shifts. This idea is corroborated by additional measurements on Fe/Nb and Co/Nb bilayers, which clearly show T_c changes related to specific magnetic domain configurations with a T_c maximum in the magnetically saturated state of the FM layer. Complementary micromagnetic simulations, delivering also the magnitude of stray fields, support the picture of influencing T_c by controlling and switching domain configurations.

DOI: 10.1103/PhysRevB.74.094504 PACS number(s): 74.45.+c, 74.62.−c, 75.60.Ch

I. INTRODUCTION

Guided by the extremely successful developments in the field of giant magnetoresistance (GMR),[1] which is based on the observation that the electrical resistance R of a stack of ferromagnetic (FM)/nonferromagnetic/FM metallic layers strongly depends on the relative orientation of the magnetization of the sandwiching FM layers, it appeared as a natural extension to substitute the intermediate normal-conducting metal by a superconducting layer (SC). Such an approach immediately leads into the field of proximity effects describing the mutual influence of the usually antagonistic effects of ferromagnetism and superconductivity. Like in a GMR arrangement including the special variant of substituting the non-FM metallic layer by a thin insulator (I) leading to the tunneling magnetoresistance (TMR), FM/SC/FM proximity trilayers or FM/I/SC/I/FM multilayers are expected to exhibit resistance changes when the relative magnetization orientation of the FM layers are changed independent of whether the transport measurements are performed with current in plane (CIP) or perpendicular plane (CPP), though in GMR experiments CPP turned out to be more effective. Resistance changes of a superconducting system at temperatures close to but below the thermodynamic transition temperature to superconductivity T_{c0} immediately are reflected in corresponding shifts of the experimentally determined superconducting transition temperature T_c as given e.g., by the midpoint temperature $T_{c,\mathrm{mid}}$ defined by $R(T_{c,\mathrm{mid}})=0.5R_0$ (R_0 is the residual resistance just above the superconducting transition). Independent, however, of this experimentally motivated T_c definition, theories dealing with FM/SC/FM proximity structures have clearly predicted T_c shifts by switching the relative magnetization orientation. Intuitively, most intriguing among these theories are those expecting higher T_c values for antiparallel (AP) as compared to parallel (P) orientations of the FM layer magnetizations, i.e., $T_c^{AP}>T_c^P$.[2–4] Indeed, corresponding spin-switching devices allowing switching between the normal and superconducting state have been suggested ("Tagirov switch")[5] pointing also to the high potential for applications of the above idea. The theoretical achievements related to the proximity effect have recently been reviewed in detail.[6] The theoretical description changes, however, if the close FM/SC proximity is lifted either deliberately by adding thin intermediate insulating layers as in a TMR-like arrangement or by naturally occurring interface barriers. In such a case, a spin-injection picture appears more appropriate and a corresponding theoretical model for FM/I/SC/I/FM layers delivers a spin accumulation for the AP orientation leading to pair breaking with an accompanying T_c depression while practically no effect on T_c is found for the P orientation, i.e., $T_c^P>T_c^{AP}$.[7–9] The related resistance changes behave like the standard GMR, i.e., a resistance enhancement in the AP orientation, as compared to P magnetizations. Thus, the qualitative results deduced from this model are just opposite to those of the proximity theories. In a more recent extension of the theory it was demonstrated that the spin-accumulation effect is still present even without the insulating interlayer, though the overall spin-dependent signals are strongly reduced in this case.[8] Experimentally, in most studies thin layers of conventional superconductors like Nb or Pb were used sandwiched by various FM materials, including exchange-biased systems in order to extend the field range where an AP magnetization orientation can be maintained. Recently, also the resistance and T_c behavior of a $La_{0.7}Ca_{0.3}MnO_3/YBa_2Cu_3O_7$ superlattice has been reported.[10] So far, however, the results obtained on FM/SC/FM trilayers or superlattices are still not conclusive, reflecting the theoretical situation with two opposite predictions with respect to the orientation dependence of T_c. For instance, for CuNi/Nb/CuNi trilayers based on the relatively weakly ferromagnetic CuNi, two experiments reported $T_c^{AP}>T_c^P$ with rather small T_c contrasts of 5 mK (Ref. 11) and 2.5 mK,[12] respectively. By substituting CuNi by the ferromagnetically stronger pure Ni, a significantly larger T_c contrast of up to 41 mK was found recently.[13] This is surprising in the context of another recent report on permalloy

($Ni_{80}Fe_{20}$,Py)/Nb/Py trilayers, which exhibited opposite behavior to what is expected by the proximity theory in that switching from *P* to AP configuration resulted in an increase of resistance when measuring the transition curve to superconductivity by a CIP arrangement.[14] The authors ascribe this observation to an enhanced reflection of spin-polarized quasiparticles at the SC/FM interface. Interface properties, which quite generally are susceptible to details of the preparation conditions, may indeed account for some of the reported controversial results. The observations reported in Ref. 14 with a standard GMR-like behavior in the superconducting state, which, however, completely disappears above T_c, are similar to those found for $La_{0.7}Ca_{0.3}MnO_3/YBa_2Cu_3O_7$ superlattices[10] and, thus, indicate that these effects are not restricted to unconventional SC or to FM materials of an especially high-spin polarization as originally supposed. While in Ref. 10 the experimentally obtained results were interpreted in terms of the spin-imbalance model mentioned above,[7] increasing experimental evidence has been provided for a completely alternative interpretation based on the domain state of the FM layers ("domain-wall superconductivity"),[15] where it is argued that the compensation of the applied field by the stray fields of the magnetic domains leads to new phenomena. Though probably more effective for domain structures of perpendicularly magnetized FM layers,[16–18] the effect has been also observed for in-plane magnetized layers.[14,19] An immediate consequence of this idea is that in order to influence the resistance or the transition temperature of a superconductor by the domain state of a nearby FM, it should be sufficient to prepare a FM/SC bilayer rather than a FM/SC/FM trilayer since the relative magnetization orientation is no longer of importance. Indeed, the studies on Py/Nb,[19] on PdNi/Nb,[20] as well as on $[Co/Pt]_{10}$/Pb, all were performed on bilayers.

In view of the somewhat unsatisfying experimental situation as outlined above, we decided to concentrate on Nb as SC and to start with Fe/Nb/Co trilayers allowing magnetization switching due to the different coercive fields of the relatively strong ferromagnetic Fe and Co layers. Emphasis is put here on the experimental determination of both the hysteretic magnetization behavior at a given temperature, and the CIP transport measurements, enabling a correlation between both properties. As will be demonstrated below, significant T_c shifts of up to 50 mK are observed with $T_c^P > T_c^{AP}$ accompanied by a standard GMR behavior, both pointing to the spin-imbalance model. Extending, however, this study to an exchange-biased system of the type Fe/Nb/Co/CoO as well as to Fe/Nb bilayers clearly reveals the decisive role of stray fields due to various domain configurations as obtained by magnetic switching. The corresponding experimental evidence will be presented after the following section on experimental details.

II. EXPERIMENTAL

The various stacks of thin multilayers used as samples in this study all were prepared at ambient temperature by pulsed laser ablation (PLD) under UHV conditions onto (001)-oriented Si substrates (size: 5×10 mm^2, *p* doped with resistivity $\rho > 3000\ \mu\Omega$ cm) using a 193 nm ArF excimer laser. Prior to film deposition, the substrates were ultrasonically cleaned in acetone and isopropanol, but no special treatments were applied to remove their native surface oxides. In PLD, the ablated plume is known to contain energetic ions up to ~200 eV, depending on the areal energy density of the laser. As a consequence, PLD is susceptible to result in interface mixing when preparing multilayers. For that reason, whenever the deposition of a new element was started, the laser power was reduced to just above the ablation threshold of this element up to a typical thickness of 1 nm before enhancing the laser power for the remaining layer deposition.[21] This enhancement is accompanied by a corresponding larger deposition rate, which is necessary to minimize the incorporation of impurities. In case of our FM/SC/FM trilayer, this translates into (13 J/cm^2, 0.75 nm/min, 5 nm Co)//(7 J/cm^2, 0.25 nm/min, 1 nm; 13 J/cm^2, 0.9 nm/min, 27.5 nm Nb)//(4.5 J/cm^2, 0.3 nm/min, 1 nm; 13 J/cm^2, 1.1 nm/min, 4 nm Fe) where information is given as (laser energy density, deposition rate, total thickness deposited at this rate, element). Since the GMR is known to be sensitive to the interface structure, the above ablation recipe has been successfully tested on Co/Cu/Co multilayers in a previous study[22] demonstrating the presence of a GMR. Presently, all multilayers are capped by a 5 nm thick Au layer to prevent oxidation. During the Co, Fe, and Au depositions a pressure of 7×10^{-9} mbar was maintained, which could even be improved to 4×10^{-10} mbar during the Nb growth by predepositing Nb onto a shutter and exploiting the resulting getter effect. Special care was taken to obtain a precise thickness measurement of the various layers by using two quartz balances, one which could moved exactly to the substrate position, allowing a calibration against externally measured layer thicknesses, and a second one at a fixed position, which is calibrated versus the first one and allows a rate and/or thickness control during deposition. More details on the PLD apparatus are given in Refs. 22 and 23.

To enable CIP transport measurements on the multilayers prior to their deposition, separate current and voltage contacts were prepared by PLD of 30 nm Au through a suitable mask. On top of these contacts the multilayers are deposited through a second mask, defining their position and lateral dimension (width 0.3 mm, length of voltage drop 3 mm). The complete arrangement is shown as the lower right inset to Fig. 1.

A remark is in order also on the superconducting properties of the Nb layers, which are known to sensitively depend on thickness,[24] as well as structural disorder[25] and impurities like oxygen.[26] In the present case of PLD, Nb layers, which were deposited at a rate of 1.2 nm/min up to a thickness above 60 nm at ambient temperature, exhibited a polycrystalline structure with a preferential (110) orientation, rocking widths between 3.2° and 4.9° full width at half maximum (FWHM) as determined by x-ray diffraction, and T_c values of typically 7.6±0.1 K. Reducing the thickness to the standard value between 20 and 30 nm resulted in the expected further decrease of T_c to values depending systematically on the corresponding deposition rate. For instance, a 20 nm thick Nb layer deposited at a rate of 0.17 nm/min showed $T_{c,\mathrm{mid}} = 3.8$ K with a residual resistance ratio *r*

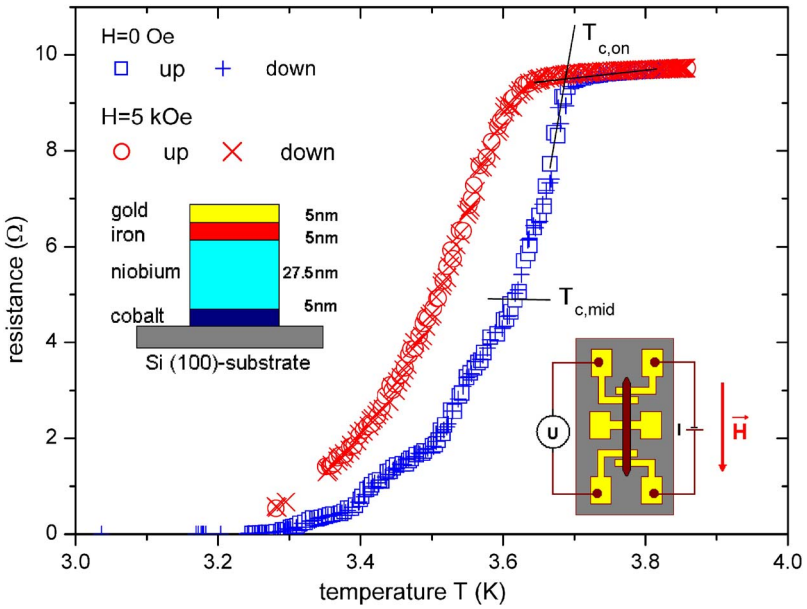

FIG. 1. (Color online) Resistively determined transitions into the superconducting state of a Co/Nb/Fe trilayer, as given in the left inset with and without an external in-plane magnetic field (values and symbols are given as upper left inset).

$=R(300\ \mathrm{K})/R(9.5\ \mathrm{K})=1.20$, while increasing the rate to 0.93 nm/min resulted in $T_{c,\mathrm{mid}}=6.3$ K and $r=1.70$. This trend indicates a combined effect of structural disorder and impurities, which, at this point, however, cannot be further distinguished. It should also be noted that for the present range of Nb thicknesses between 20 and 30 nm, any possible Neél coupling of the FM layers via the Nb interlayer will be damped out and can be safely ignored.[27]

An important experimental issue in the present study is the control and constancy of the sample temperature during the magnetoresistance measurements (in all cases with a current of $I=100\ \mu$A), which is guaranteed to within ±3 mK, as well as an optimized thermal coupling of the sample to its holder. The latter point is demonstrated in Fig. 1, where resistive transitions to superconductivity are presented with and without an external magnetic field. The field orientation relative to the sample arrangement is given in the lower right; while the stacking sequence of this sample is shown in the upper left inset. Each transition curve has been determined for decreasing (crosses) and increasing (open symbols) temperatures. The excellent agreement between the two corresponding data sets proves the good thermal coupling.

III. RESULTS AND DISCUSSION

A. Trilayer systems

We start by presenting the results obtained for the standard Co/Nb/Fe trilayers. To allow comparison between the magnetic and transport properties, in a first step the magnetic hysteresis of such a stack (details given in Fig. 2 as the inset) is determined at 5 K with a commercial SQUID magnetometer (MPMS, Quantum Design), with the magnetic field being in plane with the multilayers. The resulting hysteresis curve is given in Fig. 2 and clearly displays a two-step behavior, reflecting switching of the magnetization orientation related

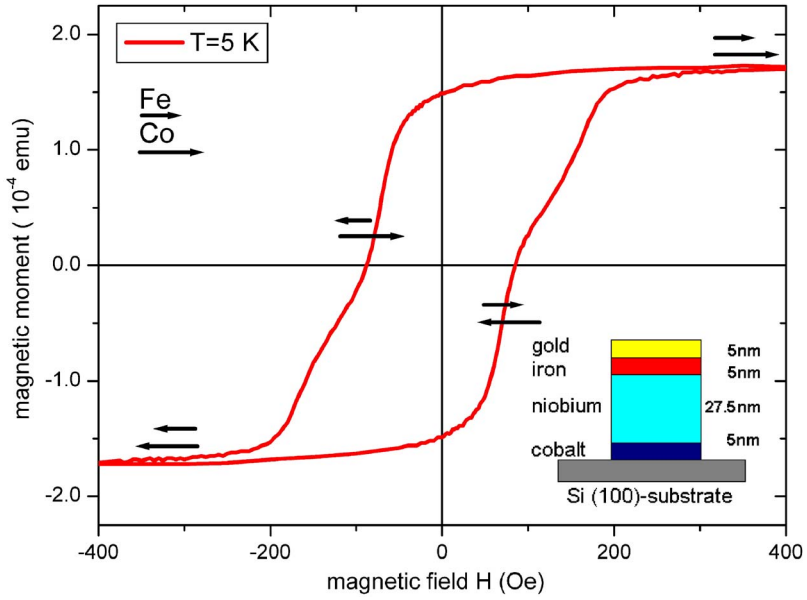

FIG. 2. (Color online) Hysteresis curve taken at 5 K of a Co/Nb/Fe trilayer, as given in the right inset. The relative orientations of the FM layers are indicated by the arrows attached to the different parts of the curve.

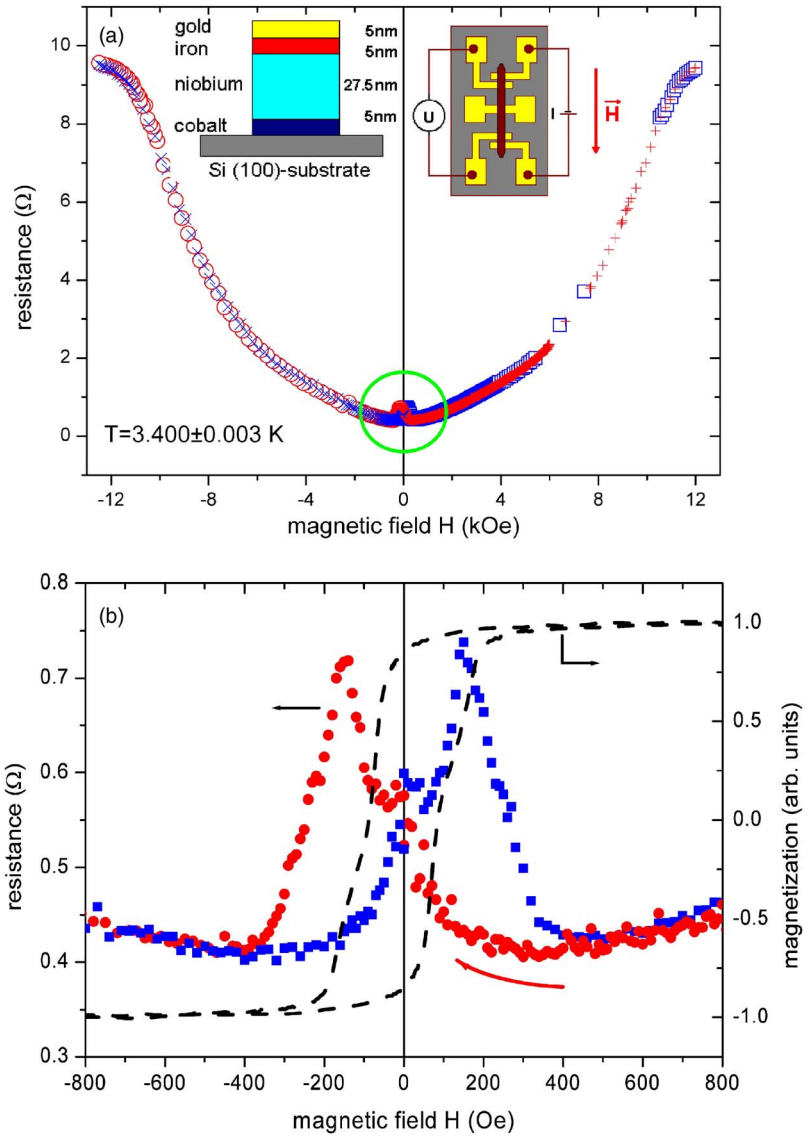

FIG. 3. (Color online) (a) Magnetic field dependence of the resistance of a Co/Nb/Fe trilayer as given in the upper left inset determined at a fixed temperature of 3.4 K and over a large field range. A complete field cycle was determined in the following sequence: ++ from +12 kOe to $H=0$, ○○ from $H=0$ to −12 kOe, ×× from −12 kOe to $H=0$, □□ from $H=0$ to +12 kOe. (b) Enlarged view of the low-field anomaly encircled in panel (a). The corresponding hysteresis is added as a dashed curve (right scale).

to the two different coercive fields H_{coe} for Fe (80 Oe) and Co (150 Oe). The relative magnetization orientations of the two sandwiching ferromagnetic layers are displayed by the two arrows added to the hysteresis curve.

Next, the magnetotransport properties of such a trilayer is analyzed in an Oxford 5T cryostat at a fixed temperature of 3.400±0.003 K, sweeping the in-plane magnetic field over a relatively large range from −12 to +12 kOe. The resulting $R(H)$ curve is presented in Fig. 3(a), where open symbols and crosses indicate field sweeps from negative to positive polarity and vice versa, respectively. At high fields, the resistance approaches its normal conducting value R_0 (cf. Fig. 1) and taking the field at $R_0/2$ as an estimate for the upper critical field H_{c2} in parallel geometry, one arrives at $H_{c2}=4.5$ kOe at a reduced temperature $T/T_{c,\mathrm{mid}}=0.94$, in reasonable agreement with previously reported values for comparable multilayers.[28,29] Thus, while an overall resistance decrease for reduced magnetic fields corresponds to the standard behavior of superconductors, a significant anomaly is visible at small magnetic fields [encircled in Fig. 3(a)]. It should be noted that the measurement temperature of 3.4 K, though being below $T_{c,\mathrm{mid}}$, is still above the "down-set temperature," resulting in a small but finite resistance even at $H=0$. By zooming into the anomaly, the results of Fig. 3(b) are obtained, where the solid circles represent resistance data (left scale) taken from positive towards negative fields, while those taken in the opposite direction are given by solid squares. When these data are overlaid by the related magnetic hysteresis curve (dashed curve, right scale), it becomes immediately clear that the resistance hysteresis closely resembles those of the standard GMR effect with a maximum resistance for AP and a minimum for P alignment of the Fe and Co magnetizations, respectively. Since an enhanced resistance represents a step towards reentrance into the normal state, one expects a slightly depressed T_c value for AP as compared to P magnetizations opposite to what is expected for the proximity, but still in agreement with the spin-imbalance model. To test this further, the temperature dependence of the switching effect was analyzed with results presented in Fig. 4. Here, the logarithmic resistance scale should be noted allowing overview of all data within the range $3.2\ \mathrm{K} \leq T \leq 3.65\ \mathrm{K} = T_{c,\mathrm{mid}}$, i.e., in the superconducting regime. Clearly, the GMR-like structure at small magnetic

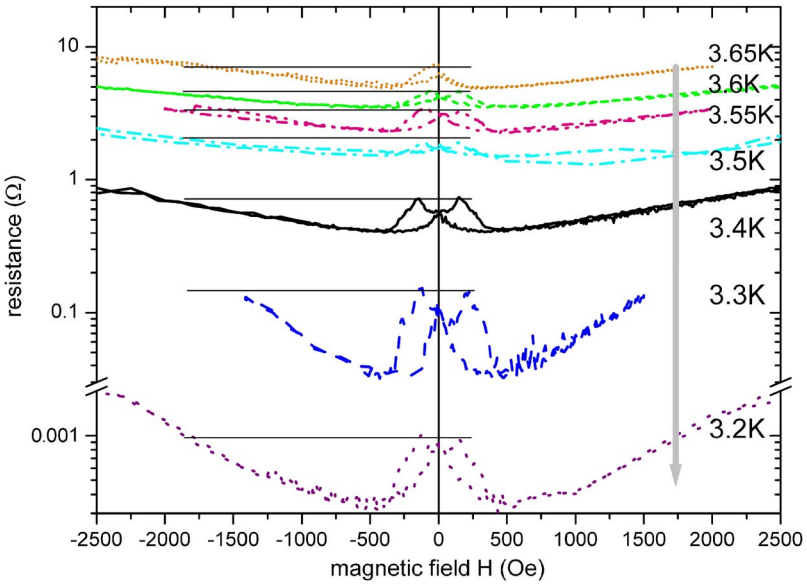

FIG. 4. (Color online) Low-field resistance anomaly of a Co/Nb/Fe trilayer at different temperatures (values attached to each curve). Note the logarithmic resistance scale.

fields strongly decreases in magnitude when the temperatures are lowered. In the context of the spin-imbalance model such a behavior can be immediately related to the decreasing number of excited quasiparticles, which exclusively are able to carry a spin current. It is interesting to note that the horizontal solid lines in Fig. 4 indicating the height of the GMR-like anomalies at low magnetic fields all cut the $R(H)$ curves at approximately the same field value of 1.7 kOe. Thus, a given magnetic field of this value parallel to the film plane would drive our superconducting system into the same resistive state as the yet-unidentified mechanism leading to the low-field anomaly. Assuming the anomaly as being due to local stray fields from the sandwiching FM layers, the above value of 1.7 kOe delivers at least an estimate of the necessary magnitude of such fields. We postpone this point, however, until discussing the behavior of bilayers.

Here, a remark concerning the spin-diffusion length $l_{S,Nb}$ within the Nb layer appears appropriate. Though $l_{S,Nb}$ for a given layer certainly depends on preparational details like structural defects and impurities, an order of magnitude estimate can be obtained by referring to a more recent experimental study on sputtered Nb films of variable thickness performed at 4.2 K.[30] In this work, a value for $l_{S,Nb}$, as determined by CPP measurements between 20 and 25 nm is given, i.e., a value close to the thickness of our Nb layers, which, on the other hand, should not depend on whether the sample is in the normal or superconducting state.[8] If $l_{S,Nb}$ is larger than the Nb layer thickness, one would expect a GMR effect as well, at a temperature just above T_c. To test this, magnetoresistance measurements were performed at 4.0 K, which justifies the assumption of identical $l_{S,Nb}$ values within the present temperature range $3.2\ \mathrm{K} \leq T \leq 4.0\ \mathrm{K}$. Thus, attributing the above low-field GMR-like anomaly to a spin diffusion by quasiparticles with $l_{S,Nb}$ larger than the Nb thickness, the data shown in Fig. 5 come as a surprise. Applying the identical measurement geometry as above, i.e., in-plane magnetic field $\vec{H}$ parallel to current density $\vec{j}$, instead of resistance maxima, much smaller minima of the order of $\Delta R/R \approx 3 \times 10^{-4}$ are observed. Furthermore, when rotating the sample by 90° to orient the in-plane field perpendicular to $\vec{j}$, these minima switch into maxima of the same order of magnitude, as can be seen from the lower half

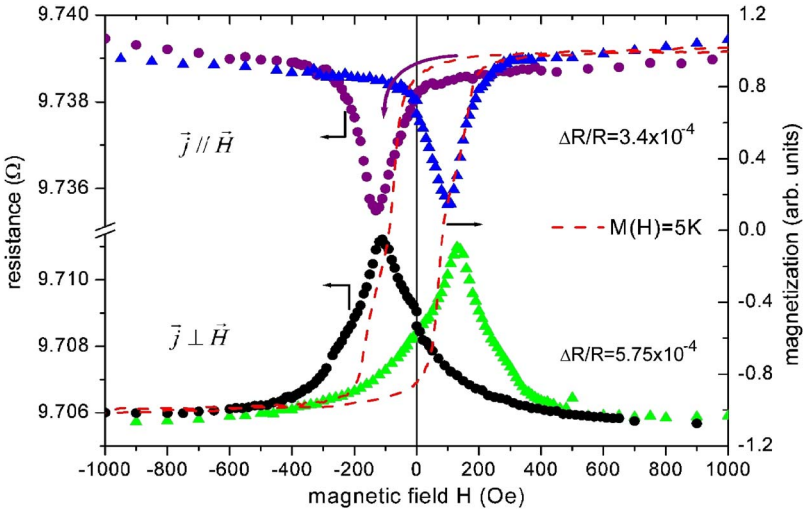

FIG. 5. (Color online) Magnetic-field dependence of the resistance of a Co/Nb/Fe trilayer measured at 4.0 K, i.e., just above T_c in the normal conducting state. Complete field cycles were determined for the current parallel (upper data points) as well as current perpendicular (lower data points) to the in-plane field. The corresponding hysteresis is added as a dashed curve (right scale).

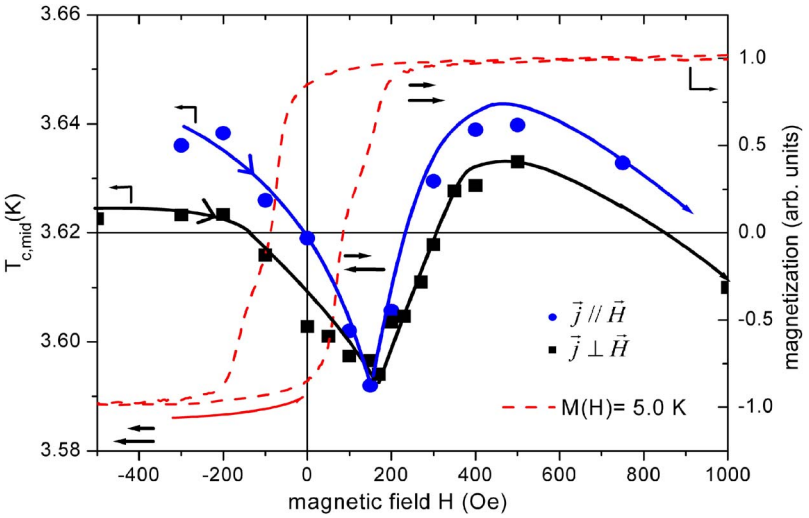

FIG. 6. (Color online) Superconducting transition temperature $T_{c,\mathrm{mid}}$ of a Co/Nb/Fe trilayer as a function of the magnetic field within the low-field range determined for two orientations of the in-plane field relative to the measurement current. The corresponding hysteresis is added as a dashed curve (right scale).

of Fig. 5. Such a behavior is characteristic of the conventional anisotropic magnetoresistance (AMR), for which a sign change is expected for the two field-current orientations. In the present case of two FM layers, the AMR should, in principle, reflect the saturation behavior of both. Due to the similar coercive fields of Fe and Co, however, and the averaging effect of the CIP geometry, the two contributions from Fe and Co cannot be resolved separately. In any case, the experiments described so far clearly demonstrate that the GMR-like anomaly is unequivocally related to the superconducting state. In this respect, the present data obtained on a conventional system are in analogy to the results reported by Peña *et al.* on $La_{0.7}Ca_{0.3}MnO_3/YBa_2Cu_3O_7$ superlattices,[10] which are interpreted in terms of the spin-imbalance effect by these authors. This analogy becomes complete by including the related T_c behavior which is given in Fig. 6. There, the experimental $T_{c,\mathrm{mid}}$ values are presented as a function of the magnetic field $\vec{H}$ (left scale) for two relative orientations, $\vec{j}$ parallel (closed dots) and perpendicular (closed squares) to $\vec{H}$ (the solid lines through these data points serve just as a guide to the eye, with the arrows indicating the direction of the field sweep). To allow relating the observed T_c changes to the magnetization state of the trilayer, the corresponding hysteresis curve is added to Fig. 6 as a dashed loop. Starting from large negative-field values corresponding to a parallel orientation of the FM magnetizations, the decrease of the field magnitude to zero, followed by a field reversal and increase of its magnitude, clearly results in continuously decreasing T_c values until a pronounced minimum is obtained, when the antiparallel magnetization orientation has been completed. Further increase of the field magnitude accompanied by orienting the magnetization parallel results in a recovery of the T_c values, which approach the same level at complete parallel orientation, as obtained for the opposite field at the starting point. For even larger fields, of course, the standard T_c depression sets in as already demonstrated above in Fig. 1. It may be worth noting that the observed T_c data are independent of the relative orientation between the magnetic field and the current direction.

Thus, the present results explicitly confirm the conclusions already drawn in the context of the resistance behavior as given in Fig. 3(b) that T_c is highest for a parallel magnetization orientation consistent with the spin-imbalance model, but opposite to the predictions related to the proximity theories. Due to the similar values of the coercive fields of Fe and Co, however, the attribution of the T_c values to magnetization orientations and switching fields still appeared too imprecise in the data presented so far. For that reason, an exchange-biased system of the type CoO/Co/Nb/Fe/Au was prepared, providing a significantly enhanced field range with an antiparallel magnetization orientation. This is demonstrated in Fig. 7, where the corresponding hysteresis curve taken at 5 K is presented (right scale), which exhibits the asymmetric behavior relative to $H=0$ characteristic of the exchange-bias effect. Here, the smaller magnetization steps occurring at smaller field magnitudes correspond to switching the Fe magnetization, the subsequent larger steps to those of Co. The resulting orientations are indicated by the two arrows attached to the corresponding parts of the hysteresis curve. Next, the T_c behavior of this system was determined and the results are included in Fig. 7 as closed dots (left scale) with the solid curve serving as a guide to the eye. Starting then at high positive fields with both magnetizations parallel, by reducing the field towards zero and changing its direction, one approaches the well-defined switching field for the Fe magnetization. Right at this switching field, T_c reaches its minimum, still in agreement with its previous attribution to the antiparallel orientation. A first inconsistency, however, with an interpretation of the T_c behavior in terms of a unique relation to the magnetization orientation, turns up when the magnetic field is further reduced while keeping the antiparallel magnetizations fixed. In the present case, as long as the antiparallel orientation is fixed, T_c is expected to conserve its minimum value. Opposite to this expectation, however, the transition temperature exhibits a steep increase immediately after switching into the antiparallel state until a maximum is obtained approximately halfway on the antiparallel magnetization plateau with a value corresponding roughly to the starting T_c in the parallel orientation. Further increase of the field leads to a continuous T_c depression as expected for "high" fields without any resolvable interruption of continuity at the second switching into the parallel magnetization state. These results strongly suggest that processes which are

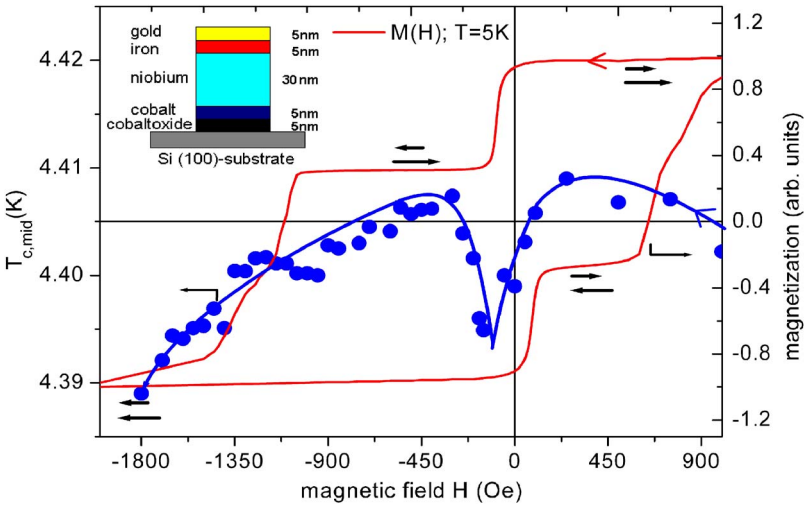

FIG. 7. (Color online) Superconducting transition temperature $T_{c,\mathrm{mid}}$ (closed dots, left scale) and magnetization taken at 5 K (right scale) as a function of the magnetic field for an exchange-biased system as given in the upper left inset. The solid curve through the T_c data points serves as a guide to the eye.

immediately related to the switching of magnetizations, rather than their relative orientation, are responsible for the observed T_c behavior. An obvious test of whether the different magnetization orientations are of essential importance for the T_c changes is to analyze FM-SC bilayers instead of the above FM/SC/FM trilayer systems. The corresponding results will be presented in the following section.

B. Bilayer systems

The following considerations and experiments are based on the idea that local stray fields resulting from a given domain state of a FM layer may induce a resistive state within the neighbored SC layer. Within this picture, a FM/SC/FM trilayer may be more effective in suppressing superconductivity or may allow us to observe this effect in even thicker SC layers; however, in principle, for its occurrence a FM-SC bilayer should be sufficient. In any case, as has been estimated in the context of Fig. 4, the necessary local stray fields should exhibit magnitudes well above 1.8 kOe to induce the experimentally observed resistances. It is also intuitively clear that these stray fields will originate from domain walls within the FM layer. Consequently, in the magnetically saturated state, stray fields are expected to be negligibly small, while close to the coercive field their effect might be largest. In this way, the observed T_c changes are traced back to the switching of domain configurations representing different distributions of local stray fields. To elaborate on this idea more quantitatively, micromagnetic simulations, based on solving the Landau-Lifshitz-Gilbert equation, were performed with the OOMMF software.[31] For this purpose, the behavior of a 5 nm thick Fe layer was simulated in two dimensions (2D) assuming a basic cell of $(10\times10\times5$ nm) and values for the magnetocrystalline anisotropy $K_1=5.2\times10^4$, $K_2=-1.8\times10^4$ (unit: J/m^3) at 4.2 K, exchange constant $A=20.7$ pJ/m, and saturation magnetization $M_S=17\times10^5$ A/m as appropriate for bulk bcc Fe.[32] Simulation of a hysteresis cycle and comparison to the experimental curves showed that an enhancement of K_1 by 20% to 5.8×10^4 J/m^3 resulted in a better agreement. Thus, in the following this larger value was adopted.

Some significant conclusions can be drawn from the results given in Fig. 8, where the upper panel represents a top view onto a 2D Fe layer ($1\ \mu\mathrm{m}\times2\ \mu\mathrm{m}$), which first was saturated by an in-plane field in the x direction, then brought into the remanent state and finally, after field reversal, to the presented state at an applied field of 75.4 Oe close to the coercive field with a magnetization of $M/M_S=+0.53$. Here, each arrow indicating the local magnetization direction represents an average over ten basic cells used for the simulation. The shadowed areas arise due to encoding the magnetization directions in a gray scale and, thus, can be qualitatively interpreted as domains. For a given simulated in-plane magnetization, the magnitude and the perpendicular

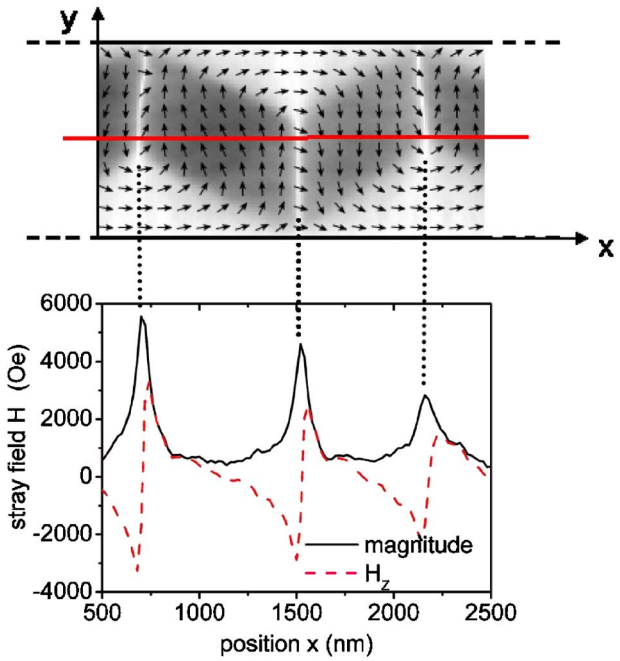

FIG. 8. (Color online) (Upper panel) Simulated magnetic domain configuration for a $1\ \mu\mathrm{m}\times2\ \mu\mathrm{m}\times5$ nm Fe layer (details are given in the text). (Lower panel) Magnitude and perpendicular component of the stray field calculated for the given domain configuration at a distance of 10 nm above the central line included in the upper panel. Vertical dots indicate the position of the domain walls.

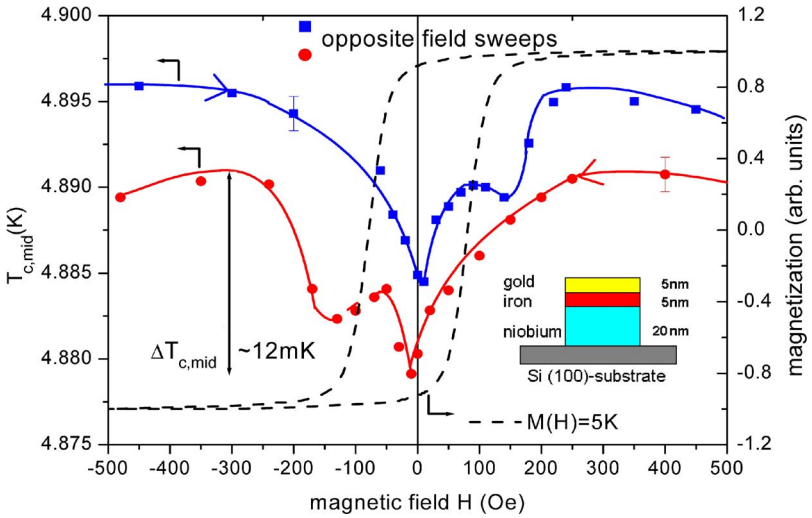

FIG. 9. (Color online) Superconducting transition temperature $T_{c,\mathrm{mid}}$ (closed dots and squares represent opposite directions of the field sweeps, as given by the arrows) as a function of the magnetic field for an Fe/Nb bilayer as shown in the lower left inset. Solid curves through the data points serve as guides to the eye. The corresponding hysteresis is added as a dashed curve (right scale).

component of the resulting stray field can be calculated at a given distance from the Fe layer. This has been performed for a distance of 10 nm from the Fe layer and the corresponding results can be found in the lower panel, where the magnitude (solid curve), as well as the perpendicular component (dashed curve) of the stray field, is plotted along the x direction, as indicated in the upper panel by the solid line at the center of the layer. Note that both panels in Fig. 8 share a common x scale. As expected, the peaks of the stray field coincide with the position of the domain walls, as marked by the vertical dotted lines. Furthermore, even though the external applied field in the simulation is only 75.4 Oe, the local stray-field components exhibit values well above the necessary estimated thresholds to induce a local resistive state within the nearby SC layer.

To experimentally test the possibility of influencing the superconducting state by stray fields from a nearby multidomain FM layer, the T_c behavior of a (5 nm Fe/20 nm Nb) bilayer was analyzed as a function of the applied magnetic field. The corresponding results are presented in Fig. 9 for a complete hysteresis cycle. Starting with a saturated Fe magnetization at negative field polarity, the solid squares give the T_c data for field changes up to Fe saturation at positive field polarity. Additionally, the closed dots describe the T_c data for the inverse direction. In both cases, the dashed curves are provided as guides to the eye. The most notable feature in these T_c data are the two minima, one close to zero field, i.e., in the remanent state, and a second close to the coercive field of Fe. For the two opposite field sweeps, these latter minima are positioned symmetrically relative to $H=0$ reflecting the corresponding Fe hysteresis curve. It should be noted that the second half cycle (closed dots) was measured one day after the first half, leading to a slight increase in the sample resistance, which, in turn, results in a 5 mK offset between the two data sets. Independent of this small drift, however, the reproducibility of the two minima leaves no doubt about their significance. This is further corroborated by two additional bilayer systems, one (5 nm Fe/22.5 nm Nb) and another one (5 nm Co/17.5 nm Nb), both delivering two T_c minima and comparable $\Delta T_{c,\mathrm{mid}}$ values of 14 and 11 mK, respectively. It is also worth mentioning that increasing the thickness of the Nb layer up to the previous standard value of 27.5 nm led to a complete disappearance of the T_c effect in bilayers. Thus, the two minima are attributed to two different domain configurations, one in the remanent state and one close to switching at the coercive field, with corresponding stray fields sufficient to influence the resistively determined T_c, while in the completely saturated state the effect on T_c vanishes. In this picture, the observed higher effectiveness of trilayer systems is simply due to the presence of stray fields at both sides of the SC layer allowing us also to use thicker Nb layers.

C. Nonmagnetized trilayer systems

In this section, one more piece of evidence is provided against the assumption that the relative magnetization orientation of the FM Co and Fe layers sandwiching a Nb layer is the decisive parameter controlling its T_c value. For this purpose, the transition temperature $T_{c,\mathrm{mid}}$ was analyzed for a 5 nm Co/40 nm Nb/5 nm Fe trilayer in the as-prepared nonmagnetized state as a function of an increasing external magnetic field. The result is shown in Fig. 10 and reveals the remarkable fact that the nonmagnetized system exhibits the lowest T_c value, which monotonously increases by approximately 20 mK by increasing the external field driving the FM layers into saturation. On field reversal, no significant T_c depression is observed in the remanent state, while close to the coercive field at negative field polarity the T_c minimum characteristic of trilayers is recovered which, however, is shallower by 10 mK, as compared to the starting situation.

IV. SUMMARY

Though the results of the last two sections provide clear evidence against the dominating influence of the magnetization orientation on the superconducting transition temperature, there are still some details, when comparing bilayer and trilayer results, which should be addressed. First, the resistance behavior found for trilayers with an example given in Fig. 3(b) exhibits two clear maxima close to the coercive fields, while in the remanent state no significant anomaly can

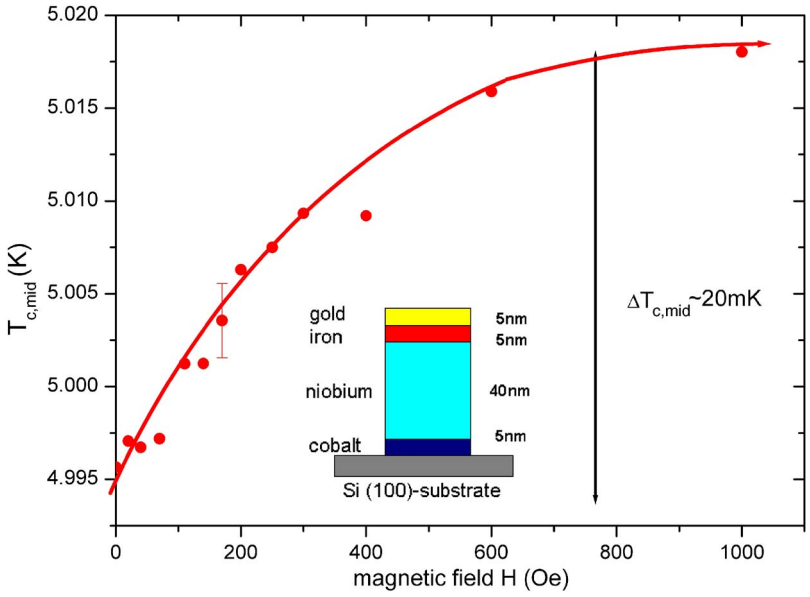

FIG. 10. (Color online) Superconducting transition temperature $T_{c,\mathrm{mid}}$ as a function of the magnetic field for the Co/Nb/Fe trilayer shown in the inset. At the starting point ($H=0$) the sample is in the as-prepared nonmagnetic multidomain state; at the end point ($H=1000$ Oe), both FM layers are magnetically saturated. The included single error bar represents the typical uncertainty when determining $T_{c,\mathrm{mid}}$ from $R(T)$ curves.

be resolved (see also Fig. 4). Similarly, the T_c behavior of trilayers is characterized by pronounced minima positioned exclusively close to the coercive fields (cf. Figs. 6 and 7). In contrast, all results on bilayers reveal an additional strong influence of the remanent state on T_c. At the moment, we have no clear experimental clue as to what is causing this difference. A possible explanation, however, could be a mutual magnetic interaction between the two FM layers, leading to a remanent state for trilayers which is much closer to saturation with a correspondingly lower density of domain walls than in the case of FM/SC bilayers. With respect to this point further experimental work appears necessary, providing especially detailed information on the various domain configurations.

Despite this complication in detail, the presented results on Fe/Nb/Co trilayers and Fe/Nb, as well as Co/Nb, bilayers, allow the clear conclusion that the standard proximity theory, with its prediction of a T_c maximum for antiparallel magnetization orientation of the sandwiching FM layers, cannot account for our experimental observations. Similarly, the spin-imbalance model, though giving the right trends of the observed resistance and T_c shifts, can be excluded, referring to the fact demonstrated in Fig. 7 that T_c strongly increases from its minimum value over a field range where the relative magnetization orientations of the FM layers are fixed in an exchange-biased system. This exclusion is then confirmed by the T_c changes induced in FM/SC bilayers, when modifying the domain configurations in the FM layer. Thus, the experimental evidence presented on controlling the transition temperature of a superconducting Nb layer by changing the magnetic state of covering FM layers is strongly in favor of an interpretation in terms of local stray fields, originating from and sensitively depending on magnetic domain configurations, which can be systematically varied along a given hysteresis cycle. These results might open the possibility to tailor superconducting properties of thin films by means of domain-wall engineering.

ACKNOWLEDGMENTS

We thank our colleagues H.-G. Boyen, A. Plettl, and J. Eisenmenger for useful discussions and technical advice, and A. Grob and R. S. Srinivasa for their help on the magnetic simulations. The financial support by the DFG Cooperative Research Center (SFB) 569 is gratefully acknowledged.

*Electronic address: paul.ziemann@uni-ulm.de

[1] E. Hirota, H. Sakakima, and I. Inomata, *Giant Magneto-Resistance Devices* (Springer-Verlag, Berlin, 2002), Vol. 40.
[2] C.-Y. You, Y. B. Bazaliy, J. Y. Gu, S.-J. Oh, L. M. Litvak, and S. D. Bader, Phys. Rev. B **70**, 014505 (2004).
[3] I. Baladié and A. Buzdin, Phys. Rev. B **67**, 014523 (2003).
[4] A. Bagrets, C. Lacroix, and A. Vedyayev, Phys. Rev. B **68**, 054532 (2003).
[5] L. R. Tagirov, Phys. Rev. Lett. **83**, 2058 (1999).
[6] A. I. Buzdin, Rev. Mod. Phys. **77**, 935 (2005).
[7] S. Takahashi, H. Imamura, and S. Maekawa, Phys. Rev. Lett. **82**, 3911 (1999).
[8] S. Takahashi and S. Maekawa, Phys. Rev. B **67**, 052409 (2003).
[9] T. Yamashita, H. Imamura, S. Takahashi, and S. Maekawa, Phys. Rev. B **67**, 094515 (2003).
[10] V. Peña, Z. Sefrioui, D. Arias, C. Leon, J. Santamaria, J. L. Martinez, S. G. E. te Velthuis, and A. Hoffmann, Phys. Rev. Lett. **94**, 057002 (2005).
[11] J. Y. Gu, C.-Y. You, J. S. Jiang, J. Pearson, Y. B. Bazaliy, and S. D. Bader, Phys. Rev. Lett. **89**, 267001 (2002).
[12] A. Potenza and C. H. Marrows, Phys. Rev. B **71**, 180503(R) (2005).
[13] I. C. Moraru, W. P. Pratt, Jr., and N. O. Birge, Phys. Rev. Lett. **96**, 037004 (2006).

[14] A. Y. Rusanov, S. Habraken, and J. Aarts, Phys. Rev. B **73**, 060505(R) (2006).
[15] Z. Yang, M. Lange, A. Volodin, R. Szymczak, and V. V. Moshchalkov, Nat. Mater. **3**, 793 (2004).
[16] W. Gillijns, A. Yu. Aladyshkin, M. Lange, M. J. Van Bael, and V. V. Moshchalkov, Phys. Rev. Lett. **95**, 227003 (2005).
[17] M. Lange, M. J. Van Bael, Y. Bruynseraede, and V. V. Moshchalkov, Phys. Rev. Lett. **90**, 197006 (2003).
[18] M. Lange, M. J. Van Bael, and V. V. Moshchalkov, Phys. Rev. B **68**, 174522 (2003).
[19] A. Y. Rusanov, M. Hesselberth, J. Aarts, and A. I. Buzdin, Phys. Rev. Lett. **93**, 057002 (2004).
[20] C. Cirillo, S. L. Prischepa, M. Salvato, C. Attanasio, M. Hesselberth, and J. Aarts, Phys. Rev. B **72**, 144511 (2005).
[21] M. Krieger, A. Plettl, R. Steiner, and P. Ziemann, Appl. Phys. A: Mater. Sci. Process. **79**, 2055 (2004).
[22] M. Krieger, A. Plettl, R. Steiner, H.-G. Boyen, and P. Ziemann, Appl. Phys. A: Mater. Sci. Process. **78**, 327 (2004).
[23] R. Steiner, H.-G. Boyen, M. Krieger, A. Plettl, P. Widmayer, P. Ziemann, F. Banhart, R. Kilper, and P. Oelhafen, Appl. Phys. A: Mater. Sci. Process. **76**, 5 (2003).
[24] S. A. Wolf, J. J. Kennedy, and M. Niesenoff, J. Vac. Sci. Technol. **13**, 145 (1976).
[25] C. Camerlingo, P. Scardi, C. Tosello, and R. Vaglio, Phys. Rev. B **31**, 3121 (1985).
[26] W. DeSorbo, Phys. Rev. **132**, 107 (1963).
[27] P. Grünberg, J. Phys.: Condens. Matter **13**, 7691 (2001).
[28] G. Verbanck, C. D. Potter, V. Metlushko, R. Schad, V. V. Moshchalkov, and Y. Bruynseraede, Phys. Rev. B **57**, 6029 (1998).
[29] T. Mühge, K. Westerholt, H. Zabel, N. N. Garif'yanov, Y. V. Goryunov, I. A. Garifullin, and G. G. Khaliullin, Phys. Rev. B **55**, 8945 (1997).
[30] W. Park, D. V. Baxter, S. Steenwyk, I. Moraru, W. P. Pratt, and J. Bass, Phys. Rev. B **62**, 1178 (2000).
[31] M. J. Donahue and D. G. Porter, OOMMF *User's Guide, version 1.2a3*, http://math.nist.gov/commf/doc/(2002).
[32] H. Kronmüller and M. Fähnle, *Micromagnetism and the Microstructure of Ferromagnetic Solids* (Cambridge University Press, London, 2003).